
SIMROUTE TECHNICAL MANUAL

SIMROUTE: A WEATHER SHIP ROUTING SOFTWARE FOR ACADEMIC PURPOSES



UNIVERSITAT POLITÈCNICA DE CATALUNYA

Table of contents

<i>SIMROUTE Technical Manual</i>	4
1. Basis and Algorithm	4
2. Waves	6
Bowditch formula	6
Following seas.....	8
Beam seas.....	8
Head seas.....	8
Aertssen formula	9
Khokhlov formula	9
Typical speed reduction curves	10
When Hs vary.....	10
When θ vary.....	11
When both θ and Hs vary	12
3. Commands	13
4. Emissions of pollutants	14
a) The initial input data	14
b) Engine power estimation	15
c) Emission Factors calculation	17

Table of figures

FIGURE 1: SAMPLE OF A NODE GRIDDED MESH.....	4
FIGURE 2: SCHEME OF THE GRID RESOLUTION, 16 EDGES PER NODE.....	6
FIGURE 3: DEFINITION OF θ	7
FIGURE 4: TYPICAL SPEED REDUCTION CURVES (PADHY, 2008).....	8
FIGURE 5: COMPARISON OF THE SPEED REDUCTION MODELS FOR $\theta = 0^\circ$	10
FIGURE 6: COMPARISON OF THE SPEED REDUCTION MODELS FOR $\theta = 90^\circ$	10
FIGURE 7: COMPARISON OF THE SPEED REDUCTION MODELS FOR $\theta = 180^\circ$	11
FIGURE 8: COMPARISON OF THE SPEED REDUCTION MODELS ACCORDING TO θ , WITH $H_s = 3\text{ m}$	11
FIGURE 9: BOWDITCH SPEED REDUCTION ACCORDING TO H_s AND θ	12
FIGURE 10: AERTSSEN SPEED REDUCTION ACCORDING TO H_s AND θ	12
FIGURE 11: KHOKHLOV SPEED REDUCTION ACCORDING TO H_s AND θ	13

SIMROUTE Technical Manual

1. Basis and Algorithm

Pathfinding or pathing is the plotting, by a computer application, of the shortest route between two points.

The two well-known pathfinding algorithms normally used are the Dijkstra Algorithm (Dijkstra, 1959) and the A* Algorithm (Dechter and Pearl, 1985). Both of them have been tested and configured in the SIMROUTE.

These pathfinding algorithms are represented through gridded meshes. The meshes are made by different points (nodes). Every single node is separated by the same distance, both horizontal and vertical axes, from the neighbouring node. Therefore, a gridded mesh is built like the following one (Grifoll et al., 2016):

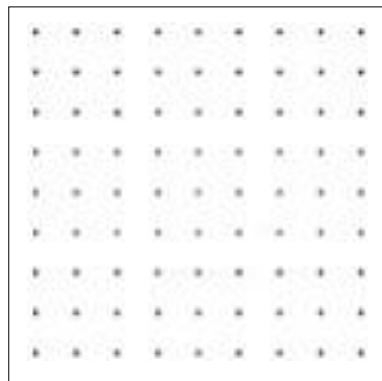


Figure 1: Sample of a node gridded mesh

To each connection (edge) a weight related to the distance is established. The great circle (orthodromic) distances are used for the spherical coordinates of the grid nodes, the same as for transoceanic pathfinding algorithms.

On the one hand, the Dijkstra Algorithm in gridded meshes picks the unvisited vertex with the lowest distance, calculates the distance through it to each unvisited neighbour and updates the neighbour's distance if smaller. Dijkstra algorithm has been used previously in ship routing applications (Mannarini et al., 2013; Montes, 2005).

On the other hand, A* algorithm finds solutions by looking at all the possible path combinations to the result (goal) for the one that obtains the minimum cost (shortest time, shortest distance travelled, etc..) and among these paths it selects the ones that appear to be the fastest to the solution. It is depicted in terms of weighted graphs: beginning from a particular node of a graph, it creates a tree of paths, expanding all these paths one node at a time, until one of the paths reaches a predestined goal node. At each repetition of its main loop, A* algorithm needs to establish which of its unfinished paths to expand into one or more longer paths (Grifoll et al., 2016).

$$f(n) = g(n) + h(n) \quad (1)$$

Where “n” is the last node on the path, $g(n)$ is the cost of the path from the start node to “n”, and $h(n)$ is a heuristic that estimates the cost of the cheapest path from n to the goal. The heuristic is problem-specific. For the algorithm to find the actual shortest path, the heuristic function must be admissible, meaning that it never overestimates the actual cost to get the nearest goal node. In the case of the study, the heuristic function is the minimum distance between origin and destination (Grifoll et al., 2016).

In the function of the grid resolution, path connection options between nodes may vary. Consequently, the sequence of edges followed by the shortest path will be limited by the grid resolution and the connected nodes. As seen in *Figure 2*, edges are connecting nodes displayed by arrows. Every single

arrow represents different potential ship courses or directions. Grid resolution can vary according to the investigator's preferences. In this work, different grid resolutions have been tested which obtained similar conclusions to that of Mannarini et al. (2013), which posited that at least 16 edges are required in order to be precise (Grifoll et al., 2016).

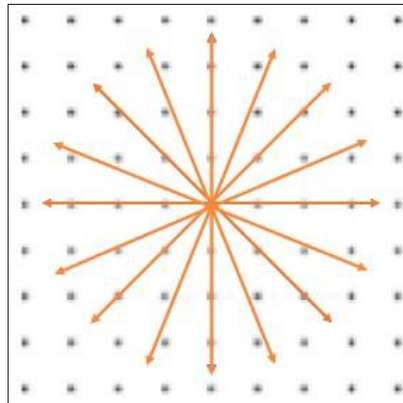


Figure 2: Scheme of the grid resolution, 16 edges per node

2. Waves

Ships can experience challenging operating conditions due to a constant action of waves. Complete knowledge of the expected sea state is important when considering vessel safety.

Wave action is the major factor that affects the ship performance and safety navigation (Hu et al., 2014). Wave fields affect ship motions by decreasing the propeller thrust and adding a resistance in comparison to absence of waves.

Bowditch formula

A simple formula to include ship speed reduction to waves is suggested by Bowditch (2002). The final speed is computed as a function of the non-wave affected speed (v_0) plus a reduction in function of the wave parameters (Grifoll et al., 2016):

$$v(H, \theta) = v_0 - f(\theta) \cdot H^5 \quad (2)$$

Where H is the significant wave height and f is a parameter in function of the relative ship wave direction. The values of f coefficient are shown in Table 1 (Grifoll et al., 2016).

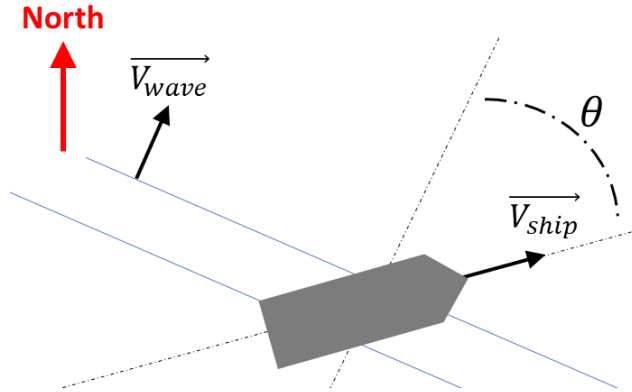


Figure 3: Definition of θ

Looking at Equation (2), one can see that the f coefficient has a significant impact on the speed of the vessel. The speed varies depending upon the wave height as well as the wave direction.

The Bowditch formula fits in the algorithm and it subtracts the speed of the vessel with the resistance of the wave in terms of height and direction.

Ship-wave relative direction	Wave direction	f (in kn/ft^2)
$0^\circ \leq \theta \leq 45^\circ$	Following seas	0.0083
$45^\circ < \theta < 135^\circ$	Beam seas	0.0165
$135^\circ \leq \theta \leq 225^\circ$	Head seas	0.0248
$225^\circ < \theta < 270^\circ$	Beam seas	0.0165
$270^\circ \leq \theta \leq 360^\circ$	Following seas	0.0083

Table 1: Values of the f coefficient

The relation of the wave direction related on ship navigation can be described as follows (Níclasen, 2010):

Following seas

There are many factors that can have a negative impact on stability and ship handling when sailing in the same direction as the waves if the waves are high compared to a vessel. The most notorious is broaching, whereby the vessel is turned violently to one side, leaving it broadside to the oncoming waves. The risk of broaching can be reduced by reducing ship speed to a fraction of the wave speed; but this again increases the risk that overtaking waves wash along upper decks from astern without this being noticed by the operators on the bridge.

Beam seas

Sailing in beam seas can result in large roll angles and, in extreme conditions, the vessel can capsize.

Head seas

Sailing against the waves is in most cases the best way to negotiate a series of large waves, but this also inflicts the most violent forces on the vessel, increasing the danger of slamming and shifting of cargo. The impact forces can be limited, to some extent, by reducing the vessel speed, or altering course.

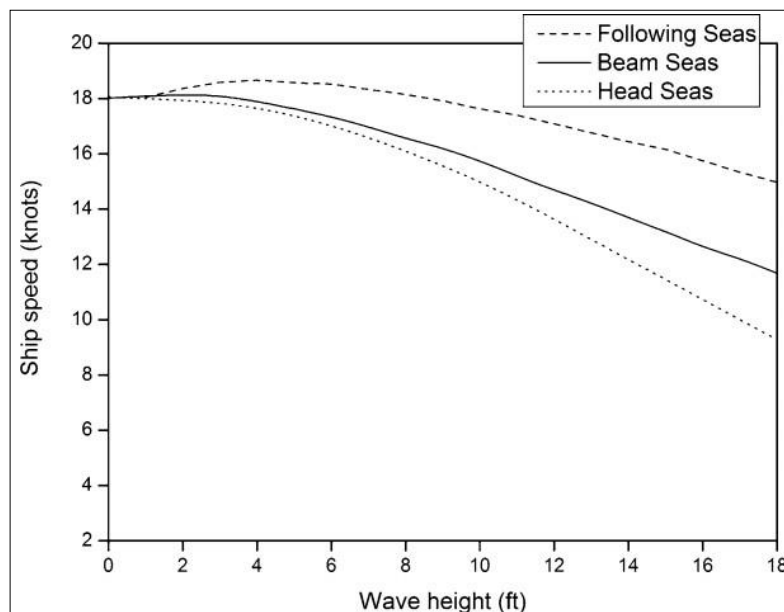


Figure 4: Typical speed reduction curves (Padhy, 2008)

Aertssen formula

This formula is suggested by Aertssen (1975). Unlike Bowditch formula, this one takes into account the ship's length between perpendiculars (Maisiuk et al., 2014):

$$v = v_0 - 6 \frac{L}{89} + n; \begin{matrix} \leq \\ >00 \end{matrix} \quad (3)$$

Where:

$L_{@A}$ length between perpendiculars [m]

m, n empirical coefficients that depend on θ . See Table 2.

θ angle between sailing direction and wave direction [deg] (Figure 3)

			$\theta \in [0^\circ-30^\circ]$		$\theta \in]30^\circ-120^\circ]$		$\theta \in]120^\circ-150^\circ]$		$\theta \in]150^\circ-180^\circ)$	
Beaufort number	Wind speed [kn]	Hs [m]	m	n	m	n	m	n	m	n
5	17-21	2.5	100	0	350	1	700	2	900	2
6	22-27	4.0	200	1	500	3	1000	5	1300	6
7	28-33	5.5	400	2	700	5	1400	8	2100	11
8	34-40	7.5	700	3	1000	7	2300	12	3600	18

Table 2: m and n coefficients according to sea state (Maisiuk et al., 2014)

Khokhlov formula

This formula is suggested by Lubkovsky (2009). It formula takes into account the vessel's dead weight, and can be applied when $4000 \leq D \leq 20000$ y $9 \leq v_0 \leq 20$ kn. According to Maisiuk et al. (2014), the standard error for this formula does not exceed 0.5 kn.

$$v = v_0 - 0,745 - 0,245 \cdot (\pi - \theta) T \cdot (1,0 - 1,35 \cdot 10^{v_0} \cdot D \cdot v_0) \cdot H_x \quad (4)$$

Where:

D vessel's dead weight [tons]

Hs waves significant height [m]

θ angle between sailing direction and wave direction [rad] (Figure 3)

This method provides similar results to Aertssen, with the advantage of providing a continuous speed reduction, while Aertssen provides a discrete reduction.

Typical speed reduction curves

When H_s vary

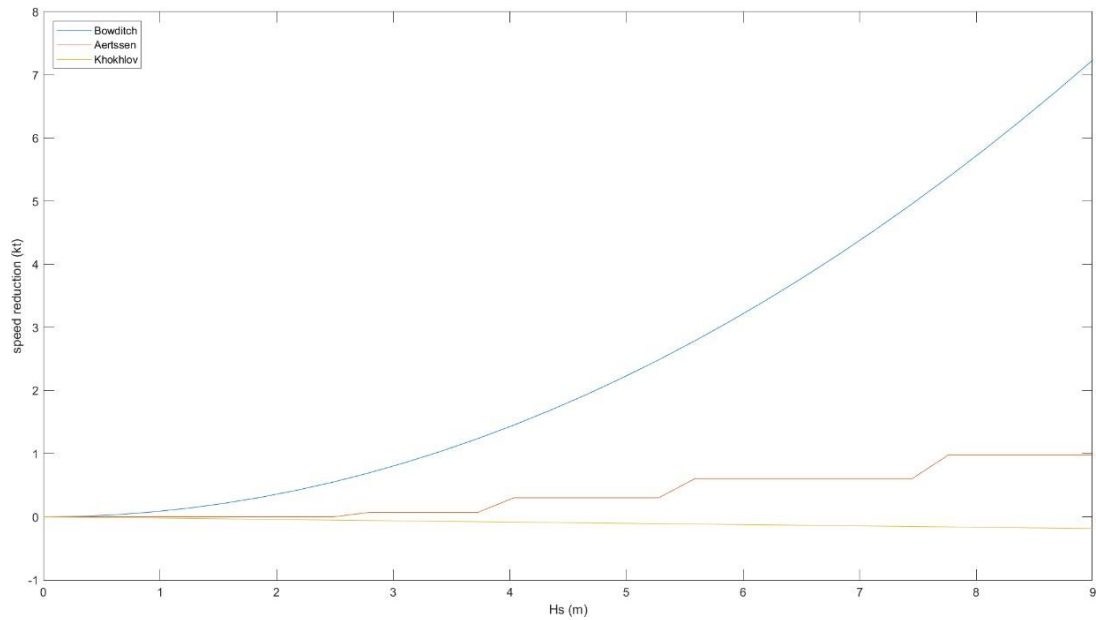


Figure 5: Comparison of the speed reduction models for $\theta = 0^\circ$.

Blue: Bowditch; Orange: Aertssen; Yellow: Khokhlov.

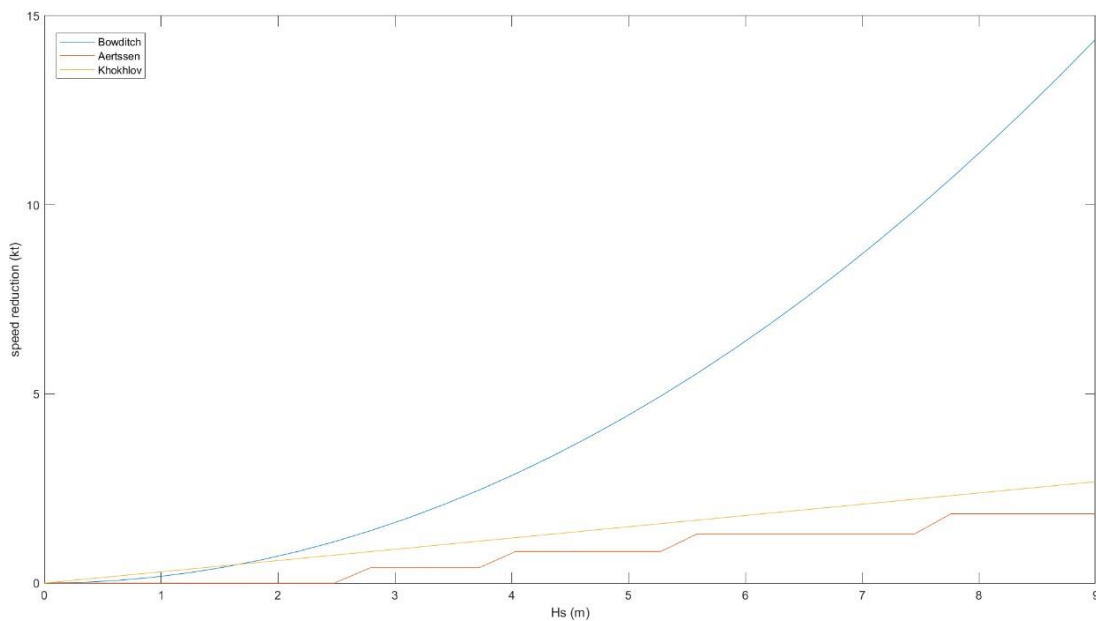


Figure 6: Comparison of the speed reduction models for $\theta = 90^\circ$.

Blue: Bowditch; Orange: Aertssen; Yellow: Khokhlov.

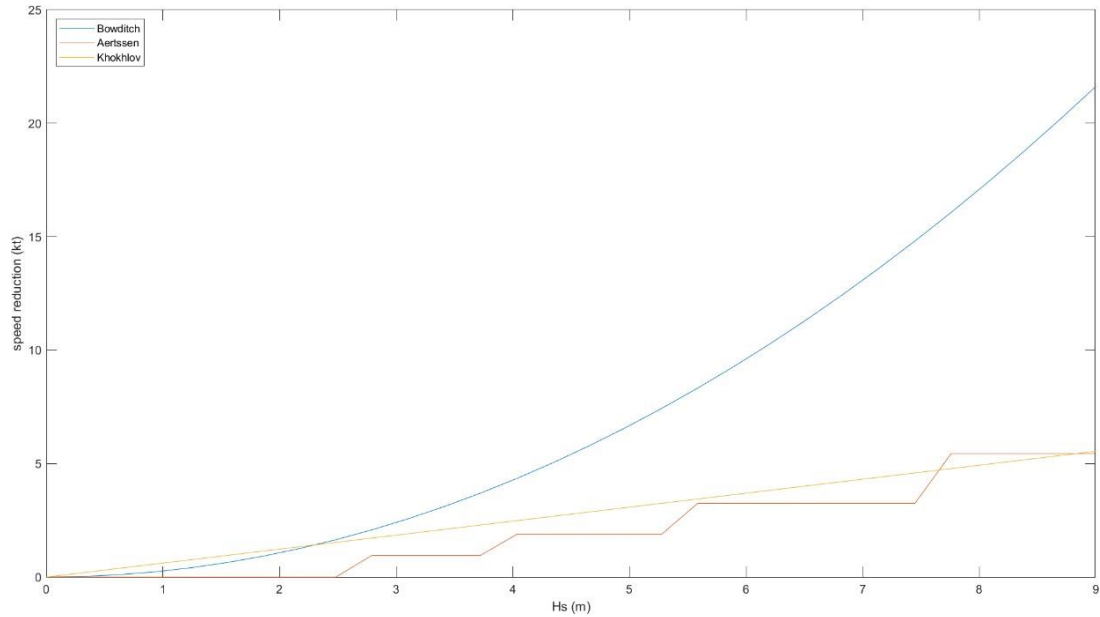


Figure 7: Comparison of the speed reduction models for $\theta = 180^\circ$.

Blue: Bowditch; Orange: Aertssen; Yellow: Khokhlov.

When θ vary

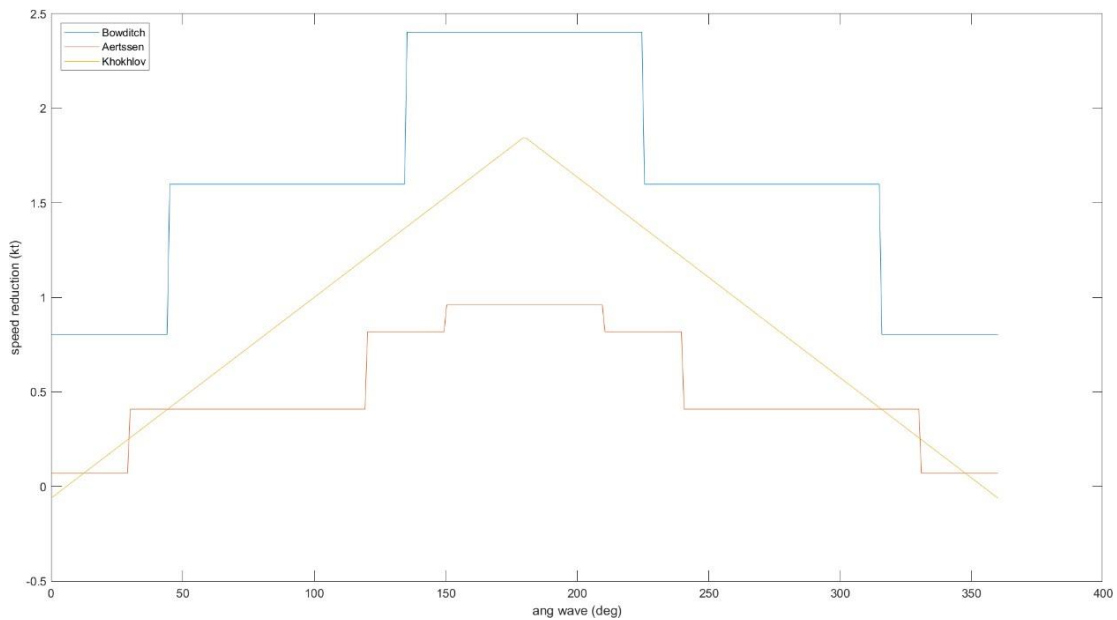


Figure 8: Comparison of the speed reduction models according to θ , with $H_x = 3$ m.

When both θ and H_s vary

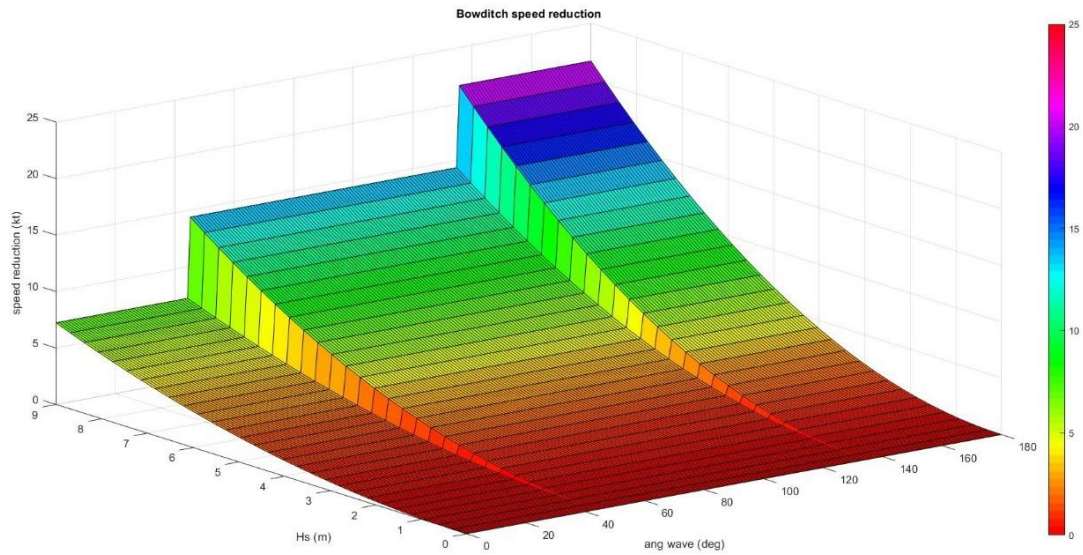


Figure 9: Bowditch speed reduction according to H_s and θ .

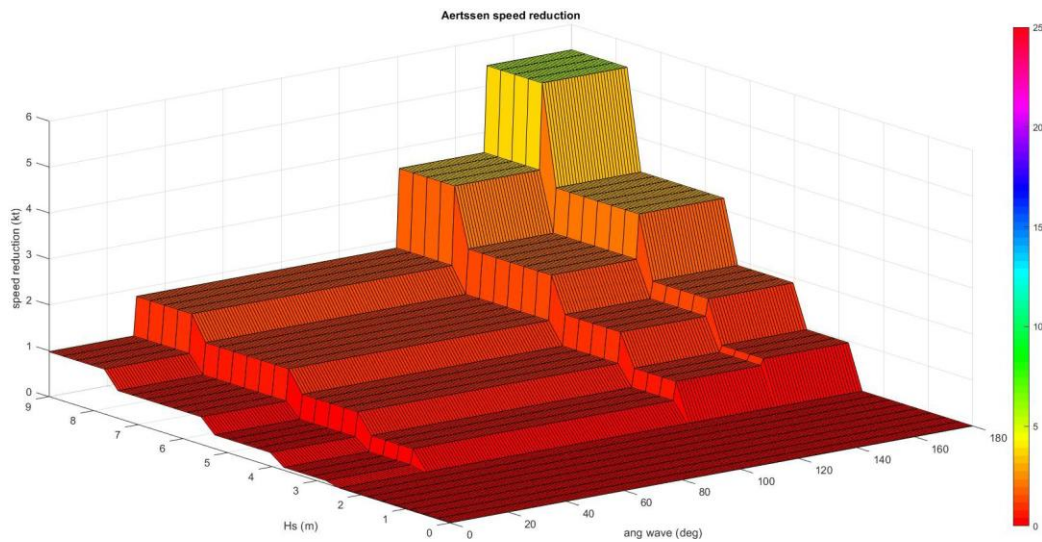


Figure 10: Aertssen speed reduction according to H_s and θ .

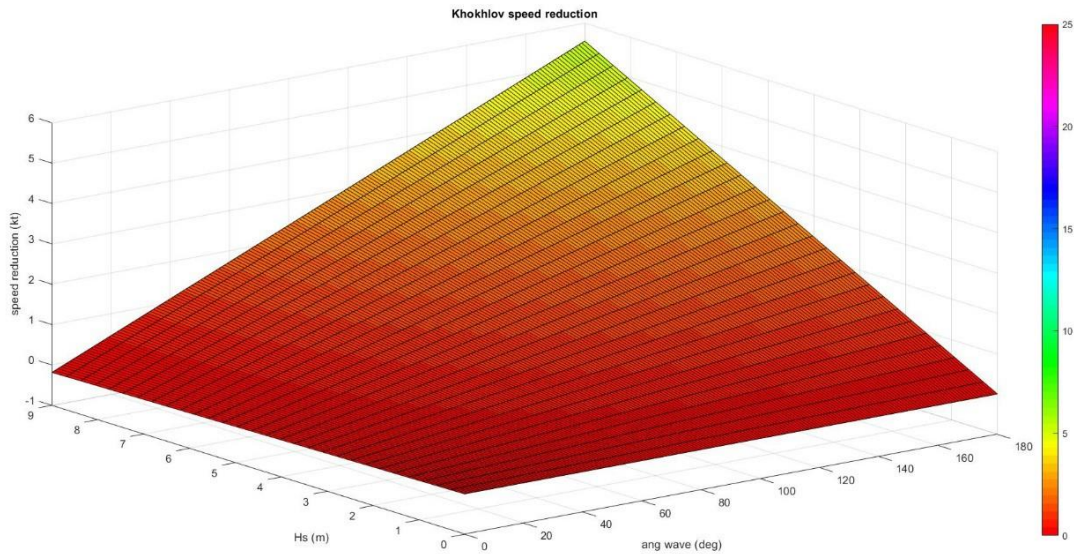


Figure 11: Khokhlov speed reduction according to H_s and θ .

3. Commands

The algorithm in Matlab possesses folders that have been previously created. In the folders, there are different files that have been made with the “.m” format in order to introduce the needed data and make them run in a concrete order. Following this paragraph, the procedure is explained:

Through the “make_mesh.m” file the corresponding latitudes and longitudes are introduced. After running the script within this file, the Western Mediterranean mesh is created.

When looking at the “make_waves.m” file, the use of the correct wave scripts has to be ensured. The wave scripts, taken from the Puertos del Estado website, have to be introduced in the file. Each script poses the waves conditions (wave height and direction) of one entire day. For instance, if the path of the route takes 80 hours and only 3 wave scripts (accounting for 72 hours) have been introduced, the algorithm will have an error. Once the correct wave scripts are introduced and the estimated time of departure (ETD) is established, an output wave script is obtained and is used for running the “simroute.m” file.

When, “simroute.m” is opened, the output script previously obtained is inserted into the file and then the initial speed of the vessel (v_0) is modified. It has to be taken into account that through the

“coord_ports.m” file the initial and end nodes (ports) for each route are created. These nodes are also introduced in the “simroute.m” file. The “simroute.m” is run and the results of the optimum route, in hours, are obtained.

Through the output scripts that “simroute.m” creates, “simroute_fix.m” can be run and the results of the shortest path route with and without waves, in hours, will be obtained (see case test of SIM-ROUTE User’s Manual).

4. Emissions of pollutants

This module has been developed for obtaining the amount of sulphur dioxide (SO₂), carbon dioxide (CO₂), nitrogen oxides (NO_x) and particulate matter (PM) generated per trip. The calculation process has been inspired by STEAM 2 methodology (Jalkanen et al., 2009).

The calculation process is described below for better comprehension:

a) The initial input data

- Installed power per engine in kW (“**Pow_Inst**”, 14400 kW as default value)
- Engine Load (“**EL**” assumed to be 80% when sailing at cruising speed)
- Design speed in knots (“**V_design**”, 25 knots as default value)
- Specific Fuel Oil Consumption in g/kWh (“**SFOC**”, 200g/kWh as default)
- Sulphur Content of fuel in mass percentage (“**SC**”, 0.027 for Fuel Oil outside ECA zones)
- Carbon Content of fuel in mass percentage (“**CC**”, 0.85 for Fuel Oil)
- Engine Revolutions per Minute (Engine_RPM, 500 rpm as default value for medium speed diesel engines)
- Molar mass of Sulphur, Sulphur dioxide, Carbon and Carbon dioxide in g/mol

The specific fuel oil consumption of 200 g/kWh is used for all engines as a default value, even though the user can change this parameter in “make_Emissions_Delta_2021” file introducing the new value as “SFOC” variable. Emissions of CO₂ and SO₂ are calculated from the fuel consumption and sulphur content, respectively (Jalkanen et al., 2009).

If engine data is unavailable, the ship is assumed to use a 500rpm medium speed diesel engine by default. Nevertheless, the user can change this parameter in “make_Emissions_Delta_2021” file by changing the value of “Engine_RPM” variable.

b) Engine power estimation

The instantaneous power can be evaluated as a function of the vessel’s speed (ITTC 1999):

$$P_{\text{shaft}} = (CF + CR + CA + CAA) \frac{v^3 S}{5} \epsilon_0 \quad (3) \quad (\text{in SI units})$$

Where:

CF	→	frictional resistance
CR	→	residual resistance
CA	→	appendage resistance
CAA	→	air resistance
ϵ_0	→	propulsive coefficient
S	→	wet surface of the ship

As above parameters are hull-specific, they cannot be found in available databases. Jalkanen et al. (2009) propose a straightforward solution assuming that they are ship-specific constants and, therefore, the power can be written as follows:

$$P_{\text{shaft}} = kv^3 \quad (4)$$

Where k is:

$$k = \frac{P_{\text{installed}}}{\varepsilon_y V_{\text{design}}^3} \quad (5)$$

Where:

$P_{\text{installed}}$	→	total installed power of main engines (kW)
ε_y	→	engine load at Maximum Continuous Rating (MCR) of main engines
V_{design}	→	design speed (m/s)

Be sure to convert m/s into knots when needed.

The emissions module takes into account the involuntary speed loss of the vessel due to waves. The effect of bad weather could be treated as (1) vessel's speed reduction for a given engine power or (2) an increase in engine power in order to maintain speed. This study considers the second option of maintaining speed in order to accomplish the Estimated Time Arrival (ETA) of the vessel. Therefore, the software calculates the increase in power (ΔP) needed to maintain the speed as a function of the speed reduction (ΔV) due to waves by the application of the following formula:

$$\frac{\Delta P}{P_{\text{installed}}} = \frac{1}{61 - \frac{\Delta V}{V}} - 1$$

Once the power increase (ΔP) is found, the new required power to maintain speed can be calculated, considering the EL_{new} and $SFOC_{\text{new}}$ for the new conditions to maintain vessel speed.

$$P_{\text{ac0}} = P_{\text{ac}} + \Delta P \quad \text{Eq. 5}$$

The same process is followed for both routes, the minimum distance and the optimized one proposed by the software.

Afterwards, the total fuel consumption (FC), converted into Tones, is calculated for the routes, using Eq.:

$$FC = \sum_{i=0}^n P_{\text{ac0}} \cdot SFOC_{\text{ac0}} \cdot t \quad \text{Eq. 1}$$

Being n the time interval and t the total time of the trip.

The procedure for calculating the emissions is described as follows:

On the first hand, the Emission Factors for the different pollutants are calculated.

An emission factor is defined as the average emission rate of a given pollutant for a given source, relative to units of activity. In this case, g/kWh.

Once the emission factors are obtained for the different pollutants, their value is multiplied by the transient power (kW), by the engine load (%) and by the duration of the trip (hours), giving as a result the amount of pollutant emitted into the atmosphere (in g, converted into Tonnes for displaying).

The process of calculation of each emission factor is described hereby.

c) Emission Factors calculation

- SO₂

SFOC = Specific Fuel Oil Consumption (g/kWh)

SC = Sulphur content of fuel (mass %)

M(S) = Molar mass of sulphur (g/mol)

m(S) = mass of sulphur (g)

M(SO₂) = Molar mass of sulphur dioxide (g/mol)

n(S) = number of moles of sulphur (mol)

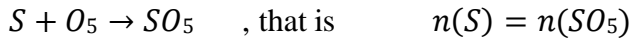
n(SO₂) = number of mols of sulphur dioxide (mol)

m(SO₂) = mass of sulphur dioxide (g)

The number of mols of sulphur are obtained by dividing the mass of sulphur (g) times its molar mass (g/mol).

$$n(S) = \frac{m(S)}{M(S)} \quad (\text{mol})$$

Bearing in mind the sulphur combustion stoichiometric formula, for a mol of sulphur burnt, there will be a mol of sulphur dioxide generated:



Furthermore, in order to find out the mass of sulphur burnt per kW in an hourly basis, the Specific Fuel Oil Consumption of the engine has to be multiplied by the Sulphur Content of the fuel burnt.

$$m(S) = SFOC * SC \quad (\text{g/kWh})$$

In order to calculate the SO_2 Emission Factor, the molar mass of SO_2 has to be multiplied by the number of mols of SO_2 and bearing in mind that $n(S) = n(SO_2)$, $n(S) = \frac{m(S)}{M(S)}$ and $m(S) = SFOC * SC$. Therefore,

$$EF(SO_2) = M(SO_2) * n(SO_2) = M(SO_2) * n(S) = M(SO_2) * \frac{SFOC * SC}{M(S)} \quad (\text{g/kWh})$$

- CO_2

The process is similar to the one followed for calculating the emission of sulphur dioxide.

SFOC = Specific Fuel Oil Consumption (g/kWh)

CC = Carbon content of fuel (mass %)

$M(C)$ = Molar mass of carbon (g/mol)

$n(C)$ = number of moles of carbon (mol)

$m(C)$ = mass of carbon (g)

$M(CO_2)$ = Molar mass of carbon dioxide (g/mol)

$n(CO_2)$ = number of mols of carbon dioxide (mol)

$m(CO_2)$ = mass of carbon dioxide (g)

$$n(C) = \frac{m(C)}{M(C)} = \frac{SFOC * CC}{M(C)}$$

$$n(C) = n(CO_5)$$

$$EF(CO_5) = M(CO_5) * n(CO_5)$$

- NO_x

The program uses crankshaft rpm (rpm, revolutions per minute) data to assign NO_x emission factors, which are based on the following (IMO, 1997):

$$\text{NOx Emission Factor (g/kWh)} = \begin{cases} 17, & \text{for engines less than 130 rpm} \\ 45.0 \cdot n^{-0.2}, & \text{for engines } 130 < n < 2000, n = \text{engine rpm} \\ 9.8 & \text{for engines over 2000 rpm} \end{cases}$$

Therefore, the NO_x emission will depend on the speed of rotation of the engine. The default value is 500 rpm. Nevertheless, this value can be changed by the user at any time.

- PM

Particulate matter is divided into Elementary Carbon (EC), Organic Carbon (OC), Ash, Sulphate (SO₄) and associated water (H₂O).

According to Jalkanen (2009), a linear regression to the data presented by Buhaug et al. (2009) can be applied, giving the following emission factor dependencies:

$$EF_{PM_{10}} = 0.312S$$

$$EF_{PM_{2.5}} = 0.244S$$

Where S is the fuel sulphur content in percentages.

$$OC_{ie} = \begin{cases} 3.333, & EL < 0.15 \\ \frac{a}{b + c \cdot EL}, & EL \geq 0.15 \end{cases}$$

Where a, b and c are dimensionless constants (a=1024, b=47600, c=32547).

$$EF_{ie} = 0.08 \text{ g/kWh}$$

$$EF_{ee} = 0.2 \text{ g/kWh}$$

$$EF_{xt} = 0.06 \text{ g/kWh}$$

The emission coefficients for EC, OC and ash have been assumed to be independent of the sulphur content.

For the emission coefficient for OC, an additional dependency on engine load is used.

The total PM emission factor is assumed to be the sum of all above emission factors:

$$EF_{Aa} = SFOC_{i8} (EF_{aeE} + EF_{15e} + EF_{ee} OC_{i8} + EF_{ie} + EF_{sa1})$$

Where:

$$SFOC_{i8} = 0.455EL^5 - 0.71EL + 1.28$$

$$SFOC = SFOC_{i8} * SFOC_{a5} \cdot \eta_{e5} \cdot \eta_{m5}$$

It is assumed that the NOx emission factors of all engines, regardless of their year of construction, can be computed based on the IMO curve and are independent of the fuel consumption. However, the predictions of the emissions of SO₂, CO₂ and PM are based on engine-specific fuel consumption (Jalkanen et al., 2009).

Technical papers

Borén, Clara; Castells-Sanabra, Marcella; Grifoll, Manel. Ship emissions reduction using weather ship Routing optimisation. *Proceedings of the Institution of Mechanical Engineers Part M-Journal of Engineering for the Maritime Environment*. 2022. Pp: 1 ~ 16.
<https://doi.org/10.1177/14750902221082901>

Borén, C, Marcella Castells-Sanabra, and M Grifoll. 2018. “Intercomparison of Emissions Assessment Methodologies in a Short Sea Shipping Framework.” In *19th International Association of Maritime Universities Annual General Assembly, International Center for Numerical Methods in Engineering (CIMNE)*, 416–24.
http://congress.cimne.com/iamu2018/frontal/doc/Ebook_IAMU_2018.pdf.

Borén, C, L Falevitch, Marcella Castells-Sanabra, and M Grifoll. 2019. “Added Resistance Parametrizations Due to Waves in a Weather Ship Routing System.” In *International Conference of Maritime Science & Technology NAŠE MORE, International Conference of Maritime Science & Technology NAŠE MORE 2019*, 50–59.

Grifoll, Manel, Clara Borén, and Marcella Castells-Sanabra. 2022. “A Comprehensive Ship Weather Routing System Using CMEMS Products and A* Algorithm.” *Ocean Engineering* 255(March): 111427.

Grifoll, M., Martínez de Osés, F.X., 2016. A Ship Routing System Applied at Short Sea Distances. A: *Journal of Maritime Research*. Vol. XIII, núm. II, p. 3-6.

Grifoll, M., Martínez de Osés, F.X. i Castells, M., 2018. Potential economic benefits of using a weather ship routing system at Short Sea Shipping. A: *WMU Journal of Maritime Affairs* [on-line]. *WMU Journal of Maritime Affairs*, Vol. 17, núm. 2, p. 195-211. ISSN 1651-436X. DOI 10.1007/s13437-018-0143-6.

Grifoll, M. et al., 2018. Ship weather routing using pathfinding algorithms: The case of Barcelona - Palma de Mallorca. A: *Transportation Research Procedia* [on-line]. Elsevier B.V., Vol. 33, p. 299-306. ISSN 23521465. DOI 10.1016/j.trpro.2018.10.106.

De Osés, X.M., Castells, M., 2009. The external cost of speed at sea: An analysis based on selected short sea shipping routes. A: *WMU Journal of Maritime Affairs*. Vol. 8, núm. 1, p. 27-45. ISSN 16541642. DOI 10.1007/BF03195151.

References

Aertssen, G., 1975. The effect of weather on two classes of container ship in the North Atlantic. *The Naval Architect* 1975; 1:11-13.



Basiana, L., Castells, M., Grifoll, M., Martínez, F. X., Borén, C., 2017. Ship-weather routing applied to short sea distances: study of the feasibility of SIMROUTEv2 algorithm. *In: International Association of Maritime Universities Annual General Assembly. "IAMU AGA 17 - 18th International Association of Maritime Universities Annual General Assembly"*. Varna, Bulgary. P. 330-340.

Bowditch, N., 2002, The American practical navigator. National Imagery and Mapping Agency, Bethesda.

Delitala, A.M.S. et al., 2010. Weather routing in long-distance Mediterranean routes. A: *Theoretical and Applied Climatology*. Vol. 102, núm. 1, p. 125-137. ISSN 14344483. DOI 10.1007/s00704-009-0238-2.

Delft, C. et al., 2006. Greenhouse Gas Emissions for Shipping and Implementation Guidance for the Marine Fuel Sulphur Directive. A: [on-line]. p. 276.

Hinnenthal, J. i Clauss, G., 2010. Robust Pareto-optimum routing of ships utilising deterministic and ensemble weather forecasts. A: *Ships and Offshore Structures*. Vol. 5, núm. 2, p. 105-114. ISSN 17445302. DOI 10.1080/17445300903210988.

IMO. (n.d.-a)., 2016. Air Pollution, Energy Efficiency and Greenhouse Gas Emissions.

Jalkanen, J.P. et al., 2009. A modelling system for the exhaust emissions of marine traffic and its application in the Baltic Sea area. A: *Atmospheric Chemistry and Physics*. Vol. 9, núm. 23, p. 9209-9223. ISSN 16807324. DOI 10.5194/acp-9-9209-2009.

Jalkanen, J.P., 2009. A modelling system for the exhaust emissions of marine traffic and its application in the Baltic Sea area. Supplement 1: The procedure for calculating the SO_x emission factor from fuel sulphur. A: Vol. 85, núm. C, p. 1-2. ISSN 0161-8105. DOI 10.1086/599017.

Jalkanen, J.P. et al., 2012. Extension of an assessment model of ship traffic exhaust emissions for particulate matter and carbon monoxide. A: *Atmospheric Chemistry and Physics*. Vol. 12, núm. 5, p. 2641-2659. ISSN 16807316. DOI 10.5194/acp-12-2641-2012.

Johansson, L., Jalkanen, J.P. and Kukkonen, J., 2017. Global assessment of shipping emissions in 2015 on a high spatial and temporal resolution. A: *Atmospheric Environment*. Vol. 167, p. 403-415. ISSN 18732844. DOI 10.1016/j.atmosenv.2017.08.042.

Lubkovsky, V.K., 2009. Determination of wind-wave speed loss of vessels for mixed type navigation with measurement of wave parameters by means of orthogonally-linear wavemeters. Ph.D. thesis: VAK 05.22.19, No. 390890; Novosibirsk.

Maisiuk, Y., Gribkovskaia, I., 2014, Fleet Sizing for Offshore Supply Vessels with Stochastic Sailing and Service Times. A: *Procedia Computer Science* 31 (2014), p. 939-948.

Mannarini, G. et al., 2013. A Prototype of Ship Routing Decision Support System for an Operational Oceanographic Service. A: *TransNav, the International Journal on Marine Navigation and Safety of Sea Transportation* [on-line]. Vol. 7, núm. 2, p. 53-59. ISSN 2083-6473. DOI 10.12716/1001.07.01.06.

Padhy, C.P., Sen, D. i Bhaskaran, P.K., 2008. Application of wave model for weather routing of ships in the North Indian Ocean. A: *Natural Hazards*. Vol. 44, num. 3, p. 373-385. ISSN 0921030X. DOI 10.1007/s11069-007-9126-1.

Panigrahi, J.K. et al., 2012. Optimal ship tracking on a navigation route between two ports: A hydrodynamics approach. A: *Journal of Marine Science and Technology*. Vol. 17, num. 1, p. 59-67. ISSN 09484280. DOI 10.1007/s00773-011-0116-3.

Prpić-Oršić, J. et al., 2014. Influence of ship routes on fuel consumption and CO₂ emission. A: *Maritime Technology and Engineering* [on-line]. September, p. 857-864. DOI 10.1201/b17494-114.

Sen, D. i Padhy, C.P., 2010. Development of a Ship weather-routing algorithm for specific application in North Indian Ocean Region. A: *The International Conference on Marine Technology*. Vol. 50, December, p. 21-27.

Simonsen, M. H., Larsson, E., Mao, W. and Ringsberg J. W., 2015. State-of-art within ship routing. *Proceedings ASME, 34th International Conference on Ocean, Offshore and Arctic Engineering*. Volume 3: Structures, Safety and Reliability. Canada

Szlapczynska, J. i Smierzchalski, R., 2009. Multicriteria optimisation in weather routing. A: *Marine Navigation and Safety of Sea Transportation* [en línia]. Vol. 3, núm. 4, p. 423.

Takashima, K., Mezaoui, B. i Shoji, R., 2009. On the Fuel Saving Operation for Coastal Merchant Ships using Weather Routing. A: *The International Journal on Marine Navigation and Safety of Sea Transportation* [en línia]. Vol. 3, núm. 4, p. 401-406. ISSN 2083-6473

Tsujimoto, M, Hinnenthal, J., 2008. Optimum Navigation for Minimizing Ship Fuel Consumption—Investigation of Route, Speed and Seakeeping Performance. *Proceedings of the 6th Osaka Colloquium on Seakeeping and Stability of Ships*, Osaka, Japan, pp. 43–50.

Viana, M. et al., 2013. *Impact of international shipping on European air quality*. ISBN 9789292133573.

Walther, L. et al., 2016. Modeling and Optimization Algorithms in Ship Weather Routing. A: *International Journal of e-Navigation and Maritime Economy* [on-line]. Elsevier B.V., Vol. 4, p. 31-45. ISSN 24055352. DOI 10.1016/j.enavi.2016.06.004.

Wei, S. i Zhou, P., 2012. Development of a 3D Dynamic Programming Method for Weather Routing. A: *International Journal on Marine Navigation and Safety of Sea Transportation*. Vol. 6, núm. 1, p. 79-85.

Winther, M. et al., 2016. EMEP/EEA Air Pollutant Emission Inventory Guidebook 2016. A: . núm. 21, p. 1-52. DOI 10.2800/247535.

Zahng, J. and Huang, L., 2016. Optimal Ship Weather Routing using Isochrone Method on the Basis of the Weather Changes. *First International Conference on Transportation Engineering*. Chengdu, China.

Zhu, X. et al., 2016. Ship weather routing based on modified Dijkstra algorithm. A: *Mmebc*, p. 696-699.